Rahva Teknik ve Sosyal Araştırmalar Dergisi
Cilt:3, Sayı:2, 2023, Sayfa: 83-95

Rahva Journal of Technical and Social Studies
Vol:3, Issue: 2, 2023, Page : 83-95

EPIXS ile $Hf_{0.5}Mo_{0.5}NbTiZrCr_X$ (X=0,1,0.3,0.5) Refrakter Yüksek Entropili Alaşımların Radyasyon Zırhlama Potansiyelleri

Zeynep AYGÜN[1, ✉] Murat AYGÜN[2]

[1]Bitlis Eren University, Vocational School of Technical Sciences, 13100, Bitlis, Turkey
[2]Bitlis Eren University, Faculty of Science and Arts, Physics Department, 13100, Bitlis, Turkey

[1]ORCID: 0000-0002-2979-0283; [2]ORCID: 0000-0002-4276-3511

✉Sorumlu Yazar: zaygun@beu.edu.tr

Geliş tarihi: 11/01/2023 Kabul tarihi: 11/07/2023

Özet: W, Zr, Nb, Ti, Mo, Ta, Hf gibi refrakter alaşım elementlerinin oluşturduğu refrakter yüksek entropili alaşımlar, savunma, havacılık ve nükleer enerji üretim endüstrileri gibi alanlarda yaygın olarak tercih edilmektedir. İyi mekanik özellikler, yüksek sıcaklıklarda korozyon ve oksidasyon direnci nedeniyle refrakter yüksek entropili alaşımlar süper alaşımlar yerine aday olarak kabul edilebilir. Bu çalışmanın amacı, EpiXS yazılımı kullanılarak refrakter yüksek entropili alaşımların Hf0.5Mo0.5NbTiZrCrx'in (x=0.1,0.3,0.5) kütle zayıflatma katsayıları, yarı kalınlık, ortalama serbest yol, etkin atom numarası ve yığılma faktörleri gibi radyasyon zayıflatma parametrelerini hesaplamaktır. Elde edilen değerlerin tutarlılığını görmek için, iyi bilinen bir kod olan XCom ile alaşımların kütle zayıflama katsayıları da hesaplanmıştır. Cr miktarındaki artışın alaşımların zırhlama kabiliyetini azalttığı sonucuna varılmıştır.
Anahtar Sözcükler: *Radyasyon zırhlama parametreleri, RHEA, radyasyon zırhlama,*

Radiation Shielding Potentials of $Hf_{0.5}Mo_{0.5}NbTiZrCr_x$ (X=0.1,0.3,0.5) Refractory High Entropy Alloys by EPIXS

Abstract: Refractory high entropy alloys formed by refractory alloying elements, such as W, Zr, Nb, Ti, Mo, Ta, Hf are widely preferred in areas such as the defense, aerospace, and nuclear power generation industries. Due to the good mechanical properties, corrosion and oxidation resistance at high temperatures, refractory high entropy alloys can be considered as candidates instead of super alloys. The objective of this study was to calculate the radiation attenuation parameters such as mass attenuation coefficients, half value layer, mean free path, effective atomic number and buildup factors of the refractory high entropy alloys, $Hf_{0.5}Mo_{0.5}NbTiZrCr_x$ (x=0.1,0.3,0.5) by using EpiXS software. The mass attenuation coefficients of the alloys were also calculated by XCom, a well-known code, to see the consistency of the obtained values. It was concluded that the increase in the amount of Cr decreases the shielding ability of the alloys.

Keywords: *Radiation attenuation parameters, RHEAs, radiation shielding.*

1. Introduction

Refractory high entropy alloy (RHEA) is one of the subgroups of high entropy alloys (HEAs) and it has been firstly reported by Senkov et al. (2010). RHEAs are based on nine refractory elements, Mo, Nb, Ta, W, V, Hf, Zr, Ti and Cr, with high melting point (Senkov et al., 2010; Miracle and Senkov, 2017; Senkov et al., 2018; Chang et al., 2018; Yurchenko et al., 2018; Gorr et al. 2017). This type HEAs have wide application areas such as aerospace industry, the nuclear industry, the chemical process industry, and next generation nuclear reactors due to their excellent oxidation and corrosion resistance, mechanical properties and wear behavior even at high temperatures (Senkov et al. 2018; Ye et al. 2016; Dam and Shaba, 2016; Kareer et al. 2019; Ayrenk, 2020). It is significant to improve light weighted and high strength materials against hard environmental conditions for aerospace industry. Lighter refractory elements (Zr, Nb, Ti, Mo etc.) can be used instead of heavy refractory elements such as tungsten, hafnium and tantalum to produce RHEAs (Li et al., 2022). Chromium (Cr) is one of the lighter refractory elements. The existence of Cr element can reduce the density, increase the high temperature strength and creep resistance, and improve the oxidation resistance and hot-corrosion resistance at high temperatures (Gao et al., 2021).

Shielding has become an important and necessary issue as a result of the increase in radiation applications. This issue makes the investigation of the radiation protection properties of several materials the subject of many studies (Eid et al. 2022; Zeyad et al. 2022; Aygun and Aygun, 2022a; Aygun and Aygun 2022b; Sayyed et al. 2020). Chemical compositions and mechanical properties of RHEAs were widely investigated previously (Senkov et al., 2018; Chang et al., 2018; Yurchenko et al., 2018; Gorr et al. 2017; Senkov et al. 2011; Yao et al. 2017; Han et al. 2018). In the present paper, our aim is to obtain the photon attenuation parameters such as mass attenuation coefficients (MAC), half value layers (HVL), mean free paths (MFP), effective atomic numbers (Z_{eff}), exposure and energy absorption buildup factors (EBF and EABF) of $Hf_{0.5}Mo_{0.5}NbTiZrCr_x$ (x=0.1,0.3,0.5) RHEAs. For the aim of studying the radiation protection abilities of the alloys, recently developed program EpiXS (Hila et al. 2021) in the energy range 1 keV-1 GeV was used.

2. Materials and Methods

EpiXS, the windows-based application code, is one of the recently developed user-friendly programs and is based on EPICS2017 of ENDF/B-VIII and EPDL97 of ENDF/B-VI.8. The code was produced for dosimetry, photon attenuation, and shielding determination in a broad energy range 1 keV–1 GeV. It is also possible to calculate some of the parameters (HVL, MAC, Z_{eff}, N_{eff}, MFP) without the knowledge of the sample density by EpiXS code (Hila et al. 2021).

In the study, the chemical compositions of the alloys were taken from the literature (Gao et al. 2021) and are given in Table 1. Density (ρ_{mix}) of alloys is determined by the rule of mixture as follows (Xiang et al. 2019):

$$\rho_{mix} = \frac{\sum_{i=1}^{n} c_i A_i}{\frac{\sum_{i=1}^{n} c_i A_i}{\rho_i}} \tag{1}$$

ρ_i, c_i and A_i are density, atomic fraction and atomic weight of element i_{th}, respectively.

The MAC corresponds to the interaction possibility between the mass per unit area of a material and photons can be obtained by the Beer–Lambert as given in Eq. 2:

$$I = I_0 e^{-\mu t} \tag{2}$$

We can obtain MAC for any compound as follows (Jackson and Hawkes, 1981);

$$\mu/\rho = \sum_i w_i (\mu/\rho)_i \tag{3}$$

where w_i and $(\mu/\rho)_i$ are the weight fraction and the MAC of the *i*th constituent element, respectively.

HVL is the thickness which decreases the incident radiation by one half, and MFP is the average distance between two interactions of photons. HVL and MFP are obtained by the following formulas,

$$HVL = \frac{In(2)}{\mu} \tag{4}$$

$$MFP = \frac{1}{\mu} \tag{5}$$

The number of atoms which define a material containing more than one element at a given energy value is called effective atomic number (Z_{eff}) and can be calculated by Eq. 6 where σ_e is the electronic cross section as given by Eq. 7 (Manohara and Hanagodimath, 2007). σ_T is the total atomic cross section. f_i, $(\sigma_T)_i$ and Z_i in Eq. 7 are the mole fraction, atomic cross section and atomic number of the i[th] element, respectively. An interpolation given in Eq. 8 can be also used for the determination of Z_{eff}. σ_1 and σ_2 are the elemental cross sections of two elements Z_1 and Z_2.

$$Z_{eff} = \sigma_T/\sigma_e \tag{6}$$

$$\sigma_e = \sum \frac{f_i}{Z_i}(\sigma_T)_i \tag{7}$$

$$Z_{eff} = \frac{Z_1(log\sigma_2 - log\sigma_T) + Z_2(log\sigma_T - log\sigma_1)}{log\sigma_2 - log\sigma_1} \tag{8}$$

The EBF is a kind of buildup factor representing the quantity of exposure relative to air while the EABF is the other type of buildup factor for which the interested quantity is the absorbed or deposited energy in the material (Kurudirek and Kurucu, 2020). EBF and EABF can be obtained by the given equations below (Harima et al. 1986; Harima, 1993). The geometric progression (G-P) fitting parameters for the alloys are determined by using fitting parameters (ANSI/ANS, 1991) in Eq. 10. Equivalent atomic number (Z_{eq}) is an energy-dependent parameter describing the properties of the investigated materials in terms of their equivalent elements. Buildup factors can be obtained using Eq. 11 or 12 by determining $K(E,x)$ in Eq. 13.

$$Z_{eq} = \frac{Z_1(logR_2 - logR) + Z_2(logR - logR_1)}{logR_2 - logR_1} \tag{9}$$

$$F = \frac{F_1(logZ_2 - logZ_{eq}) + F_2(logZ_{eq} - logZ_1)}{logZ_2 - logZ_1} \tag{10}$$

$$B(E,x) = 1 + \frac{(b-1)(K^x - 1)}{(K-1)} \quad \text{for} \quad K \neq 1 \tag{11}$$

$$B(E,x) = 1 + (b-1)x \quad \text{for} \quad K = 1 \tag{12}$$

$$K(E,x) = cx^a + d\frac{\tanh\left(\frac{x}{X_k} - 2\right) - \tanh(-2)}{1 - \tanh(-2)} \quad \text{for} \quad x \leq 40 \text{ mfp} \tag{13}$$

The ratio (R) of Compton partial mass attenuation coefficient to total mass attenuation coefficient should be defined for the material at a specific energy. The R_1 and R_2 values indicate the$(\mu m)_{Compton}/(\mu m)_{totalratios}$ of these two adjacent elements, which have Z_1 and Z_2 atomic numbers. F is G-P fitting parameters (a, b, c, d, X_K coefficients) of the studied material, while F_1 and F_2 are the values of G-P fitting parameters identical with the Z_1 and Z_2 atomic numbers at a certain energy, respectively. E and x demonstrate primary photon energy and penetration depth, respectively. The combination of K (E, x) with x allows one to perform the photon dose multiplication and determine the shape of the spectrum.

3.Results and Discussion

The chemical compositions of RHEAs taken from literature are given in Table 1 (Gao et al. 2021) and based on the knowledge of the alloys, the radiation-matter interaction parameters were determined. Variations of the calculated MAC values versus photon energies (1keV-1GeV) are given in Fig. 1. At low (1-100keV), mid (100keV–5MeV) and high (>5 MeV) energies, MAC values decreased sharply with increasing energy, slightly changed and increased with increasing energy where the photoelectric, Compton scattering and pair production processes are dominant, respectively. The MAC values of the RHEAs were also determined by Xcom (Berger and Hubbell, 1987) in order to investigate the agreement of the obtained MAC results by EpiXS. A good conformity is observed between the EpiXS and Xcom results (Fig. 1). The MAC values of the alloys and previously studied super alloys for some energy values are given in Table 2.

Table 1. Elemental concentrations and densities of RHEAs.

RHEAs	Mo	Nb	Hf	Zr	Ti	Cr	Density
$Cr_{0.1}Hf_{0.5}Mo_{0.5}NbTiZr$	12.81	24.81	23.84	24.36	12.79	1.39	8.73
$Cr_{0.3}Hf_{0.5}Mo_{0.5}NbTiZr$	12.47	24.14	23.19	23.71	12.44	4.05	8.70
$Cr_{0.5}Hf_{0.5}Mo_{0.5}NbTiZr$	12.14	23.51	22.58	23.08	12.11	6.58	8.675

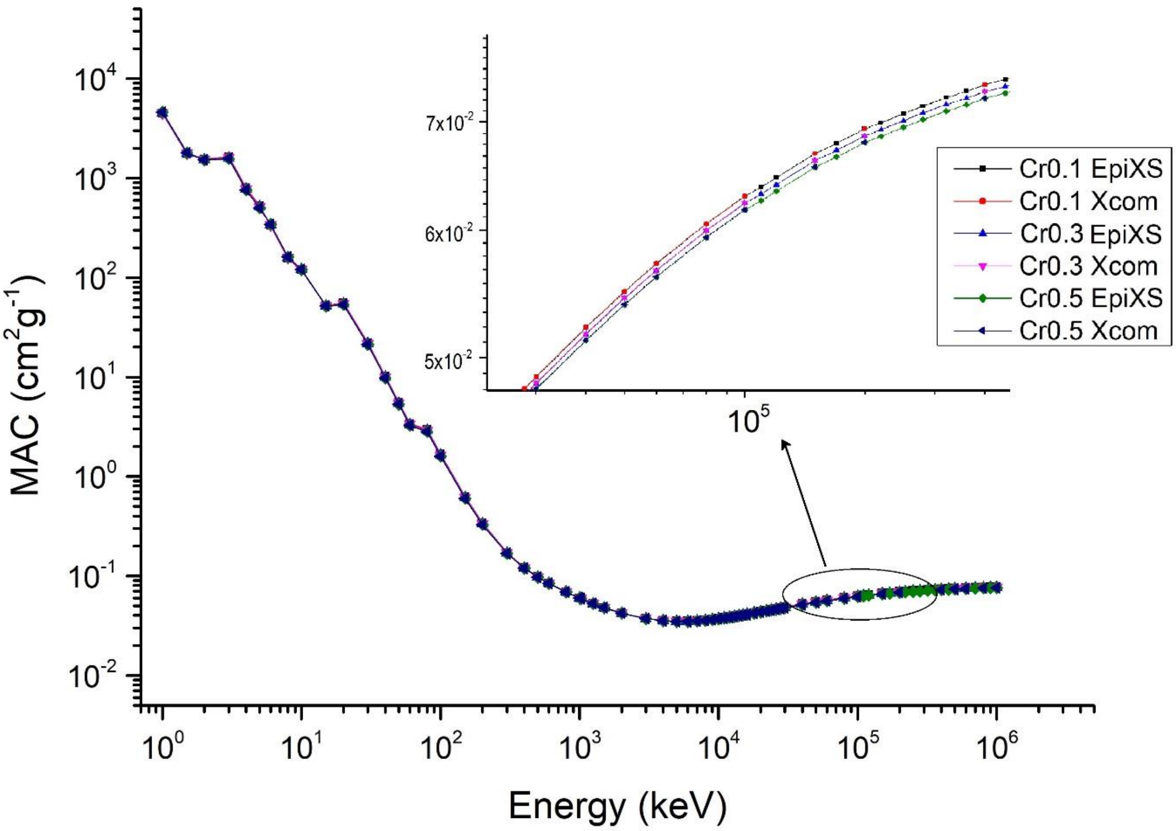

Fig. 1. Changes of MAC values of the RHEAs calculated by EpiXS and Xcom.

Table 2. MAC values of the studied alloys and previously studied samples.

Energy (MeV)	Cr0.1	Cr0.3	Cr0.5	Inc617 (Aygun and Aygun, 2022b)	Inc800HT (Aygun and Aygun, 2022b)	In625 (Sayyed et al. 2020)	In718 (Sayyed et al. 2020)	WI- (Sayyed et al. 2020)
1.50×10^{-2}	52.05	51.87	51.71	59.14	60.60	65.70	59.00	66.24
3.00×10^{-2}	22.02	21.61	21.21	10.83	8.763	9.549	10.41	9.830
5.00×10^{-2}	5.535	5.428	5.326	2.626	2.101	2.287	2.51	2.412
8.00×10^{-1}	0.068	0.068	0.068	0.068	0.067	0.068	0.067	0.068
1.00×10^{0}	0.060	0.060	0.060	0.060	0.060	0.061	0.060	0.060
3.00×10^{0}	0.037	0.037	0.037	0.037	0.036	0.037	0.037	0.036
5.00×10^{0}	0.035	0.035	0.035	0.032	0.032	0.032	0.032	0.032
8.00×10^{0}	0.036	0.036	0.036	0.031	0.030	0.031	0.031	0.031
1.00×10^{1}	0.037	0.037	0.037	0.031	0.030	0.031	0.031	0.031

The HVL and MFP are the important parameters for determining shielding capabilities of the samples. Changing of HVL and MFP values versus photon energies determined by EpiXS are given in Fig. 2. Lower HVL and MFP values are preferred to have better shielding property. According to the obtained results, HVL and MFP values of the alloy with $Cr_{0.1}$ are lower than those of others. Alloy with $Cr_{0.5}$ has the highest values of HVL and MFP. Therefore, it can be stated that $Cr_{0.1}Hf_{0.5}Mo_{0.5}NbTiZr$ has higher shielding ability than other studied alloys.

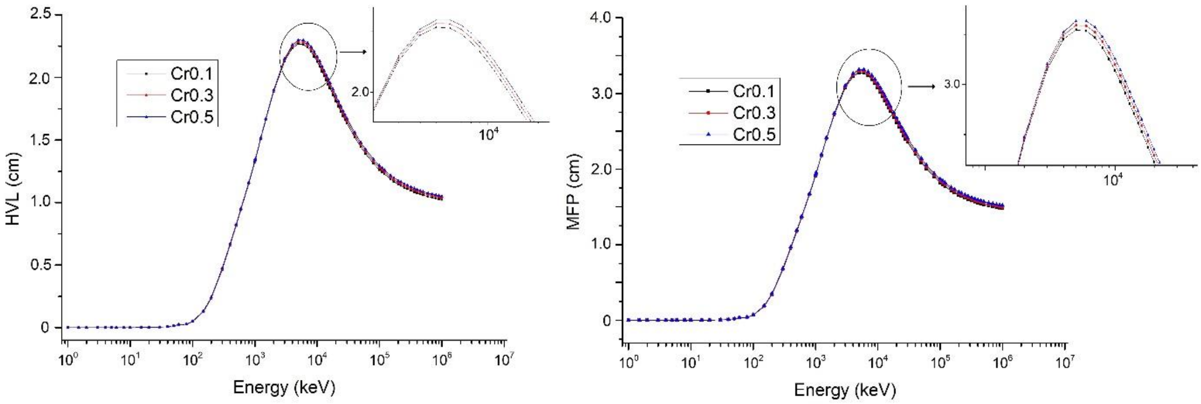

Fig. 2. Variations of HVL and MFP values of the studied alloys versus photon energies by EpiXS.

Z_{eff} variations versus photon energies obtained by the code are given in Fig. 3. K-absorption edge of Zr with 0.018 MeV is observed for Z_{eff} as seen in Fig. 3 (Abdullah et al. 2010). Z_{eff} values at around 0.019 and 0.02 MeV can be due to K-absorption edges of Nb and Mo, respectively (Sayyed et al. 2020). K-absorption edge of Hf with 0.065 MeV is also observed for Z_{eff} (Ostadhossein et al. 2022). Approximately same values were obtained for Z_{eff} parameter because of the same contents of the RHE alloys. Due to the existence of Hf, and Mo (higher atomic number), Z_{eff} values of the alloys are higher compared with the previously reported alloys.

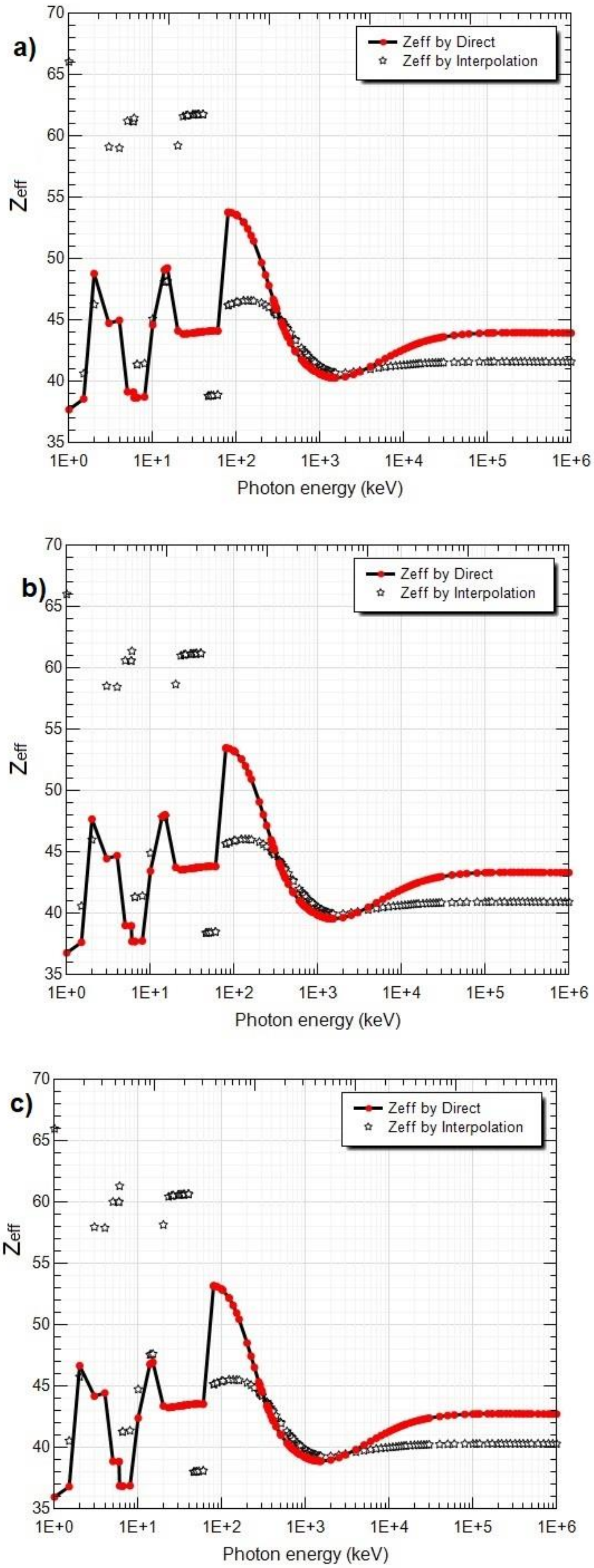

Fig. 3. Z_{eff} values of Cr0.1 (a) Cr0.3 (b) and Cr0.5 (c) alloys by EpiXS.

EABF and EBF of the studied alloys were determined for 1,2,5,10,20,30 and 40 mfp penetration depths by EpiXS. The dependences of EABF and EBF versus incident photon energies are shown in Figs. 4-5. Photoelectric effect causes the absorption of low-energy photons and so buildup factor values are small at low photon energies. Compton scattering in mid-energy region causes an increase in photon accumulation due to the large number of scattered photons and build up factors are maximum at these energies. Since the dominant process at high energies is Pair production, a strong photon absorption is observed and as a result, the buildup factors decrease at high energies (Sayyed et al. 2020; Aygun and Aygun, 2022a-c). The lowest photon cluster is observed for $Cr_{0.1}$ RHEA and so Compton scattering effect is observed for Cr0.1 at least. The maximum seen at ≈0.065 MeV can be due to K-absorption edge of Hf as mentioned above for Z_{eff} (Ostadhossein et al. 2022).

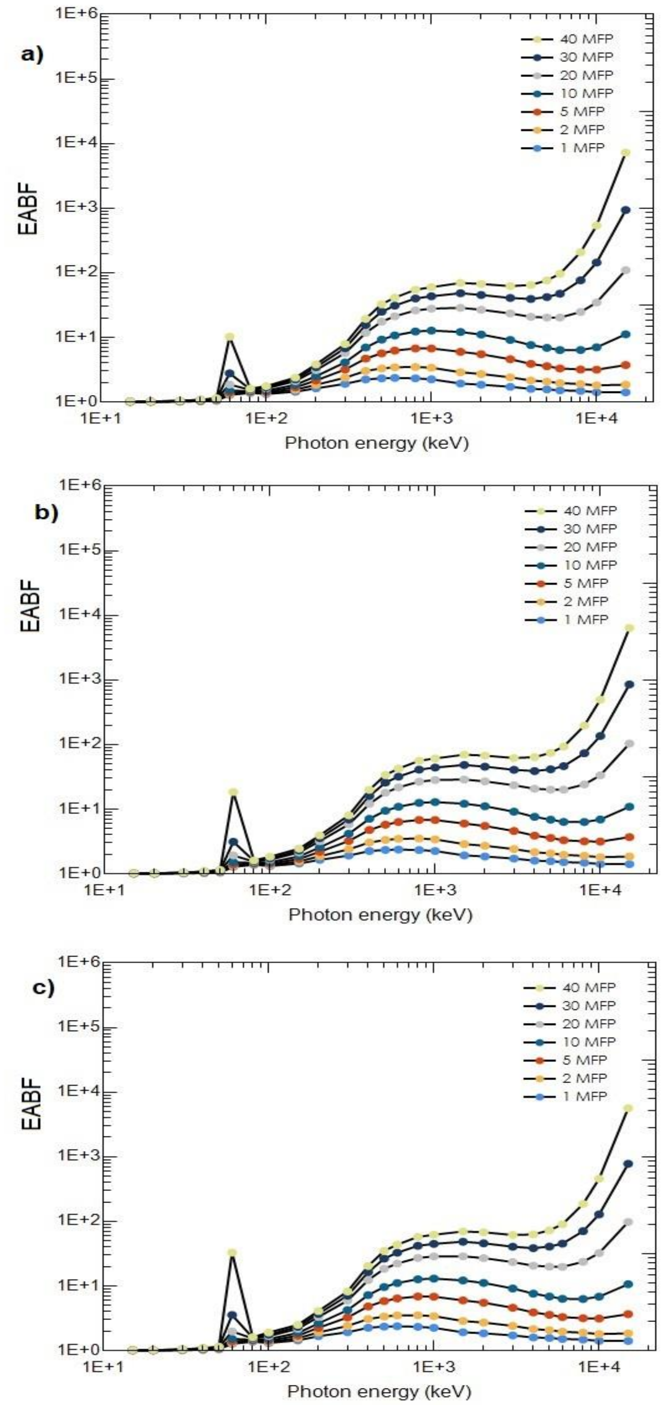

Fig. 4. EABF of Cr0.1 (a) Cr0.3 (b) and Cr0.5 (c) alloys by EpiXS.

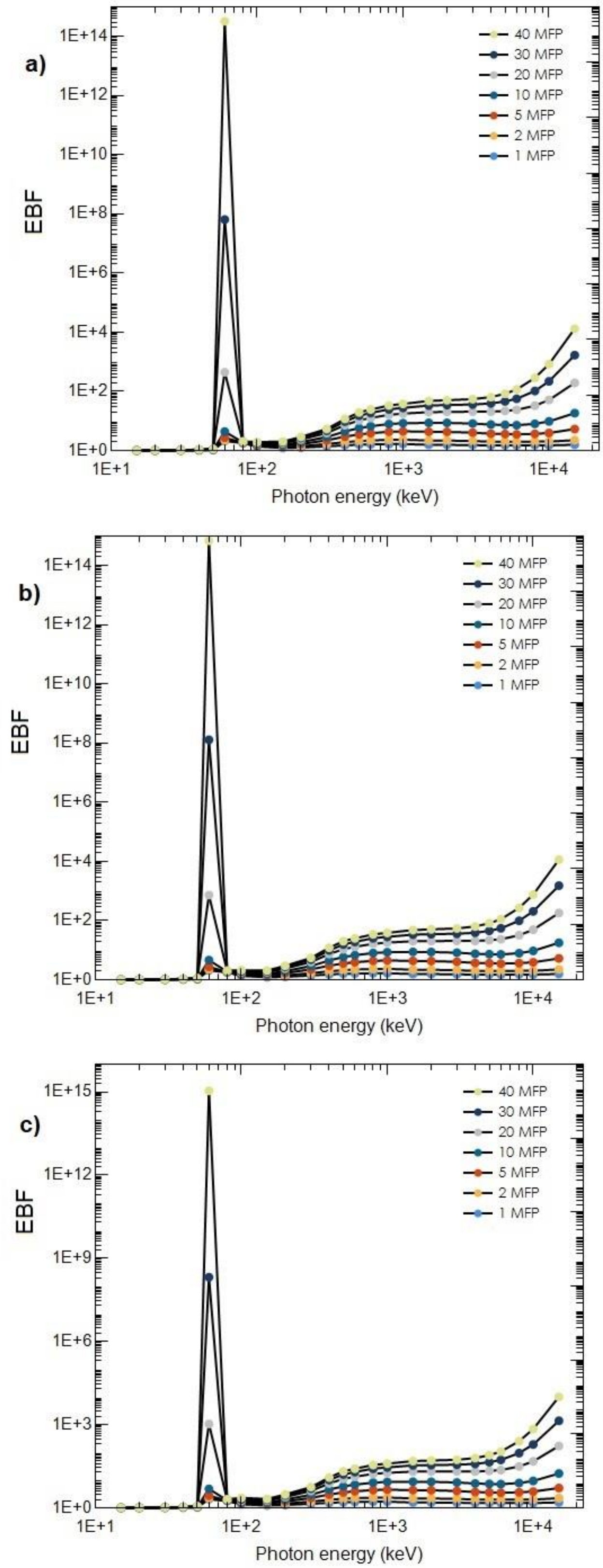

Fig. 5. EBF of Cr0.1 (a) Cr0.3 (b) and Cr0.5 (c) alloys by EpiXS.

Z_{eq} is an effective parameter on determination of energy absorption calculation and absorbed dose. While all partial photon interactions are effective for the determination of Z_{eff}, Z_{eq} is calculated only by Compton scattering (Aygun et al. 2021). The calculated Z_{eq} of the samples are given in Fig. 6. It was obtained that Z_{eq} values of Cr0.1 are higher than those of the alloys.

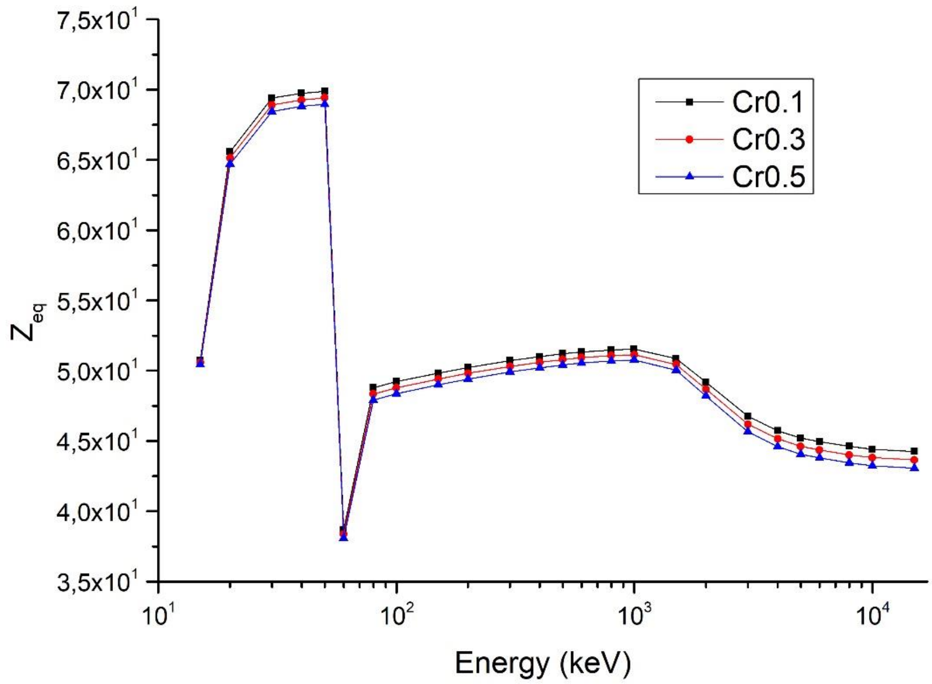

Fig. 6. Z_{eq} values of the studied RHEAs by EpiXS.

4.Conclusions

In the study, photon-matter interaction parameters of RHEAs were determined by EpiXS code in the range of 1 keV-100 GeV in order to determine how the increase in Cr concentration affects the shielding potential of the RHEAs. MAC was also determined by using Xcom and it was found that the obtained results are in good agreement. It was observed that Cr0.1 shows highest shielding capability than the others. It can be noted that increasing value of Cr concentration decreases the radiation shielding ability of the sample. This may be because of the decreasing amount of Hf and other contents (higher atomic numbers) of the alloy or density factor. Lastly, it is important to say that the studied RHEAs can be evaluated as new type shielding materials with their superior features.

Acknowledgement

The abstract text was published at the 2nd International Rahva Technical and Social Researches Congress.

Conflict of Interest

No conflict of interest was declared by the authors.

Authors Contribution

The authors declared that they contributed equally to the article.

Financial

This research did not receive any grants from any funding institution/industry

References

Abdullah, K.K., Nair, K.K., Ramachandran, N., Varier, K.M., Babu, B.R.S., Joseph, A., Thomas, R., Magudapathy, P., Nair, K.G.M. (2010). X-ray attenuation around K-edge of Zr, Nb, Mo and Pd: A comparative study using proton-induced X-ray emission and 241Am gamma rays. PRAMANA Journal of Physics, 75(3), 459–469.

ANSI/ANS 6.4.3. (1991). Gamma-ray Attenuation Coefficients and Buildup Factors for Engineering Materials. American Nuclear Society, La Grange Park, Illinois.

Aygun, Z., Yarbasi, N., Aygun, M., (2021). Spectroscopic and radiation shielding features of Nemrut, Pasinler, Sarıkamıs and Ikizdere obsidians in Turkey: Experimental and theoretical study, Ceramics International, 47, 34207-34217

Aygun, Z., Aygun, M., (2022a). Radiation Shielding Potentials of Rene Alloys by Phy-X/PSD Code. Acta Physica Polonica A, 141, 507-515.

Aygun, Z., Aygun, M., (2022b). Evaluation of radiation shielding potentials of Ni-based alloys, Inconel-617 and Incoloy-800HT, candidates for high temperature applications especially for nuclear reactors, by EpiXS and Phy-X/PSD codes, Journal of Polytechnic, 26(2), 795-801.

Aygun, Z., Aygun, M., (2022c). A study on usability of Ahlat ignimbrites and pumice as radiation shielding materials, by using EpiXS code, International Journal of Environmental Science and Technology, 19, 5675–5688.

Ayrenk, A., (2020). Synthesis and development of refractory high entropy alloys, Master thesis. Cankaya Unv.

Berger, M.J., Hubbell, J.H., (1987). XCOM: Photon Cross Sections Database, Web Version 1.2. National Institute of Standards and Technology Gaithersburg, MD 20899, USA. available at. http://physics.nist.gov/xcom.

Chang, C.H., Titus, M.S., Yeh, J.W., (2018). Oxidation Behavior between 700 and 1300 ºC of Refractory TiZrNbHfTa High-Entropy Alloys Containing Aluminum, Advance in Engineering Materials, 20(6), 1700948.

Dam, T., Shaba, S., (2016). Ductilizing Refractory High Entropy Alloys” (Bachelor’s thesis. Chalmers University of Technology). Chalmers Publication Library. http://publications.lib.chalmers.se/records/fulltext/237688/237688.pdf

Eid, M.S., Bondouk, I.I., Saleh, H.M., Omar, K.M., Sayyed, M.I., El-Khatib, A.M., Elsafi, M., (2022). Implementation of waste silicate glass into composition of ordinary cement for radiation shielding applications, Nuclear Engineering and Technology, 54(4), 1456-1463.

Gao, X.J., Wang, L., Guo, N.N., Luo, L.S., Zhu, G.M., Shi, C.C., Su, Y.Q., Guo, J.J., (2021). Microstructure characteristics and mechanical properties of Hf0.5Mo0.5NbTiZr refractory high entropy alloy with Cr addition, International Journal of Refractory Metals Hard Material, 95, 105405.

Gorr, B., Müller, F., Azim, M., Christ, H.J., Müller, T., Chen, H., Kauffmann, A., Heilmaier, M., (2017). High-Temperature Oxidation Behavior of Refractory High-Entropy Alloys: Effect of Alloy Composition, Oxidation of Metals, 88(3–4), 339–349.

Miracle, D., Senkov, O., (2017). A critical review of high entropy alloys and related concepts" Acta Materialia, 122, 448-511.

Han, Z.D., Luan, H.W., Liu, X., Chen, N., Li, X.Y., Shao, Y., Yao, K.F., (2018). Microstructures and mechanical properties of TixNbMoTaW refractory high-entropy alloys, Material Science and Engineering A, 712, 380-385.

Harima, Y., Sakamoto, Y., Tanaka, S., Kawai, M., (1986). Validity of the geometric-progression formula in approximating gamma-ray buildup factor, Nuclear Science Engineering, 94(1), 24–35.

Harima, Y., 1993. An historical review and current status of buildup factor calculations and applications, Radiation Physics and Chemistry, 41(4–5), 631–672.

Hila, F.C., Astronomo, A.A., CAM, D., Jecong J.F.M., Javier-Hila A.M.V. et al., (2021). EpiXS: A Windows-based program for photon attenuation, dosimetry and shielding based on EPICS2017 (ENDF/B-VIII) and EPDL97 (ENDF/B-VI.8), Radiation Physics and Chemistry, 182, 109331.

Jackson, D.F., Hawkes, D.J., (1981). X-ray attenuation coefficients of elements and mixtures, Physics Reports, 70, 169–233.

Kareer, A., Waite, J.C., Li, B., Couet, A., Armstrong, D.E.J., Wilkinson, A.J., (2019). Short communication: Low activation, refractory, high entropy alloys for nuclear applications, Journal of Nuclear Material, 526, 151744.

Kurudirek, M., Kurucu, Y. (2020). Investigation of some nuclear engineering materials in terms of gamma ray buildup factors at experimental energies used in nuclear physics experiments. Radiation Effects and Defects in Solids, 175, 7-8, 640-656.

Li, T., Miao, J., Lu, Y., Wang, T., Li, T., (2022). Effect of Zr on the as-cast microstructure and mechanical properties of lightweight Ti2VNbMoZrx refractory high-entropy alloys, International Journal of Refractory Metals Hard Material, 103, 105762.

Manohara, S.R., Hanagodimath, S.M., (2007). Studies on effective atomic numbers and electron densities of essential amino acids in the energy range 1keV–100GeV, Nuclear Institution Methods Physics Research Section B, 258, 321-328.

Ostadhossein, F., Moitra, P., Gunaseelan, N., Nelappana, M., Lowe, C., Moghiseh, M., Butler, A., Ruiter, N., Mandalika, H., Tripathi, I., Misra, S.K., Pan, D. (2022). Hitchhiking probiotic vectors to deliver ultra-small hafnia nanoparticles for 'Color' gastrointestinal tract photon counting X-ray imaging, Nanoscale Horizon, 7, 533–542.

Sayyed, M.I., Mohammed, F.Q., Mahmoud, K.A., Lacomme, E., Kaky, K.M., et al., (2020). Evaluation of Radiation Shielding Features of Co and Ni-Based Superalloys Using MCNP-5 Code: Potential Use in Nuclear Safety, Applied Science, 10, 7680.

Senkov, O.N., Wilks, G.B., Miracle, D.B., Chuang, C.P., Liaw, P.K., (2010). Refractory high-entropy alloys, Intermetallics, 18(9), 1758–1765.

Senkov, O.N., Wilks, G.B., Scott, J.M., Miracle, D.B., (2011). Mechanical properties of Nb25Mo25Ta25W25 and V20Nb20Mo20Ta20W20 refractory high entropy alloys, Intermetallics, 19(5), 698-706.

Senkov, O.N., Miracle, D.B., Chaput, K.J., Couzinie, J.P., (2018). Development and exploration of refractory high entropy alloys—A review, Journal of Material Research, 33(19), 3092–3128.

Xiang, C., Han, E.H., Zhang, Z.M., Fu, H.M., Wang, J.Q., Zhang, H.F., et al., (2019). Design of single-phase high-entropy alloys composed of low thermal neutron absorption cross-section elements for nuclear power plant application, Intermetallics, 104, 143-53.

Yao, H.W., Qiao, J.W., Hawk, J.A., Zhou, H.F., Chen, M.W., Gao, M.C., (2017). Mechanical properties of refractory high-entropy alloys: Experiments and modeling, Journal of Alloy and Compounds, 696, 1139-1150.

Ye, Y., Wang, Q., Lu, J., Liu, C., Yang, Y., (2016). High-entropy alloy: challenges and prospects, Material Today, 19(6), 349-362.

Yurchenko, N., Panina, E., Zherebtsov, S., Salishchev, G., Stepanov, N., (2018). Oxidation Behavior of Refractory AlNbTiVZr0.25 High-Entropy Alloy, Material, 11(12), 2526.

Zeyad, A.M., Hakeem, I.Y., Amin, M., Tayeh, B.A., Agwa, I.S., (2022). Effect of aggregate and fibre types on ultra-high-performance concrete designed for radiation shielding, Journal of Building Engineering, 58, 104960.